



AFRL-AFOSR-JP-TR-2018-0048

Minimization of Capacity Fading in Li rich $x\text{Li}_2\text{MO}_3-(1-x)\text{LiMO}_2$ Composite Cathode based on Defect and Computational Considerations

**Kuan-Zong Fung
NATIONAL CHENG KUNG UNIVERSITY**

**04/06/2018
Final Report**

DISTRIBUTION A: Distribution approved for public release.

Air Force Research Laboratory
AF Office Of Scientific Research (AFOSR)/ IOA
Arlington, Virginia 22203
Air Force Materiel Command

REPORT DOCUMENTATION PAGE				<i>Form Approved</i> OMB No. 0704-0188	
<p>The public reporting burden for this collection of information is estimated to average 1 hour per response, including the time for reviewing instructions, searching existing data sources, gathering and maintaining the data needed, and completing and reviewing the collection of information. Send comments regarding this burden estimate or any other aspect of this collection of information, including suggestions for reducing the burden, to Department of Defense, Executive Services, Directorate (0704-0188). Respondents should be aware that notwithstanding any other provision of law, no person shall be subject to any penalty for failing to comply with a collection of information if it does not display a currently valid OMB control number.</p> <p>PLEASE DO NOT RETURN YOUR FORM TO THE ABOVE ORGANIZATION.</p>					
1. REPORT DATE (DD-MM-YYYY) 24-05-2018		2. REPORT TYPE Final		3. DATES COVERED (From - To) 29 Sep 2016 to 28 Sep 2017	
4. TITLE AND SUBTITLE Minimization of Capacity Fading in Li rich xLi ₂ MO ₃ -(1-x)LiMO ₂ Composite Cathode based on Defect and Computational Considerations				5a. CONTRACT NUMBER	
				5b. GRANT NUMBER FA2386-16-1-4136	
				5c. PROGRAM ELEMENT NUMBER 61102F	
6. AUTHOR(S) Kuan-Zong Fung				5d. PROJECT NUMBER	
				5e. TASK NUMBER	
				5f. WORK UNIT NUMBER	
7. PERFORMING ORGANIZATION NAME(S) AND ADDRESS(ES) NATIONAL CHENG KUNG UNIVERSITY 1, TA HSUEH RD., TAINAN CITY, 70101 TW				8. PERFORMING ORGANIZATION REPORT NUMBER	
9. SPONSORING/MONITORING AGENCY NAME(S) AND ADDRESS(ES) AOARD UNIT 45002 APO AP 96338-5002				10. SPONSOR/MONITOR'S ACRONYM(S) AFRL/AFOSR IOA	
				11. SPONSOR/MONITOR'S REPORT NUMBER(S) AFRL-AFOSR-JP-TR-2018-0048	
12. DISTRIBUTION/AVAILABILITY STATEMENT A DISTRIBUTION UNLIMITED: PB Public Release					
13. SUPPLEMENTARY NOTES					
14. ABSTRACT Lithium-rich layered oxides have recently become attractive cathode materials for energy storage applications. Lithium-rich layered oxides, formulated as xLi ₂ MnO ₃ (1-x)LiMO ₂ in which M representing Mn, Ni or Co receive great attention for both high-power and high capacity lithium-ion cells. However, there are obstacles such as structural stabilities and capacity fading for these cathode materials to be overcome. In this study, aliovalent doping such as Mo-doping into Li-rich layered oxide was found to be able to improve the conductivity, electrochemical performance and stabilized the structure of Li-rich cathode effectively. The Mo-doped Li-rich cathode 0.5Li ₂ Mn _{1-x} MoxO ₃ -0.5LiNi _{1/3} Mn _{1/3} Co _{1/3} O ₂ was successfully synthesized through sol-gel method. The XRD pattern showed that impurity phases identified as MoO ₃ as the content of Mo increases to x=0.05. The addition of Mo induces the reduction of Mn ion from +4 to +3 and the conductivity enhancement of the Li-rich cathode. The electrochemical test showed that the Mo-doped sample exhibited the highest cycling discharge and cycling performance among the test samples. In 0.5Li ₂ Mn _{1-x} MoxO ₃ -0.5LiNi _{1/3} Mn _{1/3} Co _{1/3} O ₂ , the sample with X=0.025 exhibited 269mAh/g in the first discharge capacity and remained 224mAh/g after 30cycles. While the undoped one shows 244.5mAh/g in the first cycle and then decayed to 202mAh/g after 30cycles. The AC impedance results indicates that the R _{ct} (charge transfer resistance) was reduced after Mo-doping. Such improvement may be also the reason why the Mo-doped sample exhibited the enhanced capacity performance, in particular, at high C-rate.					
15. SUBJECT TERMS Batteries, Electrodes, Cathodes, Composites, Lithium, Energy, Mesoporous, Failure Mechanism, Modeling, Oxygen Vacancy					
16. SECURITY CLASSIFICATION OF:			17. LIMITATION OF ABSTRACT SAR	18. NUMBER OF PAGES 19	19a. NAME OF RESPONSIBLE PERSON KNOPP, JEREMY
a. REPORT Unclassified	b. ABSTRACT Unclassified	c. THIS PAGE Unclassified			19b. TELEPHONE NUMBER (Include area code) 315-227-7006

Minimization of Capacity Fading in Li rich $x\text{Li}_2\text{MO}_3-(1-x)\text{LiMO}_2$ Composite Cathode based on Defect and Computational Considerations

October 2016 –September 2017

PI and Co-PI information:

Taiwan PI: Kuan-Zong Fung, National Cheng Kung University (NCKU)

/z8702009@email.ncku.edu.tw/Department of Materials Science and Engineering/ No.1, University Road, Tainan City 701, Taiwan (R.O.C.) /886-6-2380208

Co-PI: Chia-Chin Chang, National University of Tainan (NTUT)/ Department of Greenergy

US PI: Ying Shirley Meng, University of California San Diego(UCSD)/ Laboratory for Energy Storage and Conversion / Department of NanoEngineering

Period of Performance: October /1st/2016 –September /30th/2017

Abstract:

Lithium-rich layered oxides have recently become attractive cathode materials for energy storage applications. Lithium-rich layered oxides, formulated as $x\text{Li}_2\text{MnO}_3 \cdot (1-x)\text{LiMO}_2$ in which M representing Mn, Ni or Co receive great attention for both high-power and high capacity lithium-ion cells. However, there are obstacles such as structural stabilities and capacity fading for these cathode materials to be overcome. In this study, aliovalent doping such as Mo-doping into Li-rich layered oxide was found to be able to improve the conductivity, electrochemical performance and stabilized the structure of Li-rich cathode effectively. The Mo-doped Li-rich cathode $0.5\text{Li}_2\text{Mn}_{1-x}\text{Mo}_x\text{O}_3 \cdot 0.5\text{LiNi}_{1/3}\text{Mn}_{1/3}\text{Co}_{1/3}\text{O}_2$ was successfully synthesized through sol-gel method. The XRD pattern showed that impurity phases identified as MoO_3 as the content of Mo increases to $x=0.05$. The addition of Mo induces the reduction of Mn ion from +4 to +3 and the conductivity enhancement of the Li-rich cathode. The electrochemical test showed that the Mo-doped sample exhibited the highest cycling discharge and cycling performance among the test samples. In $0.5\text{Li}_2\text{Mn}_{1-x}\text{Mo}_x\text{O}_3 \cdot 0.5\text{LiNi}_{1/3}\text{Mn}_{1/3}\text{Co}_{1/3}\text{O}_2$, the sample with $X=0.025$ exhibited 269mAh/g in the first discharge capacity and remained 224mAh/g after 30cycles. While the undoped one shows 244.5mAh/g in the first cycle and then decayed to 202mAh/g after 30cycles. The AC impedance results indicates that the R_{ct} (charge transfer resistance) was reduced after Mo-doping. Such improvement may be also the reason why the Mo-doped sample exhibited the enhanced capacity performance, in particular, at high C-rate.

Introduction:

Among energy storage devices, Li ion batteries show the highest capacities (in Ah) in all aspects. The capacity of a battery is determined by both cathode and anode used. For anodes used in Li ion batteries, graphite is the most widely used anode material. With each intercalated Li ion surrounded by six C atoms, the capacity of graphite is easily estimated to be 372 mAh/g. Recent development of other anode materials such as SnO₂, Sn alloy, Si, significantly improve the anode capacity to greater than 1000 or 2000 mAh/g. On the contrary, the cathode capacities are not only limited to an average below 150 mAh/g but also degrades with increasing cycling mainly due to its own structural instability. As a result, the weight of a Li ion battery is mainly limited by the cathode capacity. When the weight or volume of Li ion battery module becomes an important issue, to improve the capacity and cycling performance of cathode is very critical. Layered structured LiCoO₂ or LiNi_{1/3}Mn_{1/3}Co_{1/3}O₂(NMC) being the important cathode materials for many consumer electronics and auto applications, still exhibit far less capacity than anode due to the limitation of high Li delithiation and corresponding structure distortion or change. To solve this problem, an idea of excess Li source as the reservoir of Li was proposed by Lu et al. [1]. A composite lithium rich layered oxide cathode material (xLi₂MO₃- (1-x)LiMO₂, M = Mn, Co, Ni, Cr), The Li [Li_(1/3-2x/3)Ni_xMn_(2/3-x/3)] O₂ (0 <x <0.5) system showed very high capacity greater than 250mAh /g [2-3]. The research reported by Bo Xu et al [4] shows that the presence of Li₂MnO₃ is important to stabilize the MO₂ blocks in high capacity composite layered material xLi₂MO₃-(1-x) LiMO₂ through the rearrangement of Li ions in the transition metal layer as shown Fig.1(a). As the lithium ions move out of the lithium layer in a layered structure, the lithium ions located in transition metal layers tend move to the tetrahedral sites to stabilize the lithium layered structure. The schematic diagrams are shown in the following Figs.1(b) and (c). However, Li-rich layered composite cathode still exhibit obstacles, such as capacity fading, to be overcome. Based on the charge compensation concept in defect chemistry, electronic defects may be created by aliovalent doping in oxides. Desired electronic defects may be able to enhance the structural stability as well as cycling behavior. Thus, Mo-doping into Li-rich layered oxide was adopted to increase the electron defect and improve the conductivity, and electrochemical performance. In this study, The Mo-doped Li-rich cathode 0.5Li₂Mn_{1-x}Mo_xO₃-0.5LiNi_{1/3}Mn_{1/3}Co_{1/3}O₂ was synthesized through sol-gel method. The XRD, STEM, conductivity measurement, electrochemical testing were employed to conduct microstructural, structural and impedance analyses.

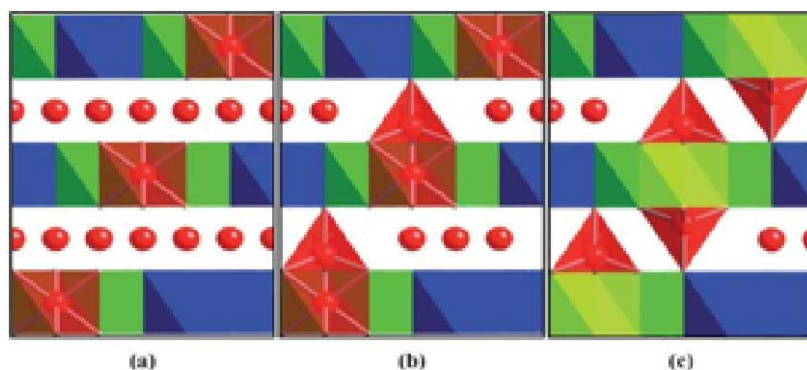


Fig.1 Sketch of Li–Li dumbbell formation (Red:Li; Green:Mn; Blue:Ni; Yellow: Vacancy). [4]

Experimental:

Powder preparation

In this study, the $0.5\text{Li}_2\text{Mn}_{1-x}\text{Mo}_x\text{O}_3-0.5\text{LiNi}_{1/3}\text{Mn}_{1/3}\text{Co}_{1/3}\text{O}_2$ ($x=0, 0.025$ and 0.5) powders were prepared by sol–gel method using citric acid monohydrate as the chelating agent. First, lithium acetate, manganese (II) acetate tetrahydrate, nickel (II) acetate hexahydrate, cobalt (II) acetate hexahydrate and ammonium heptamolybdate (as a source of Mo) were dissolved in deionized water and continuously stirred in an aqueous solution of citric acid. Subsequently, ethylene glycol was added into the prepared solution and continuously stirred. The molar ratio of total metal ions to citric acid was fixed at 1:1. The resultant solution was evaporated at 120°C to form a thicker sol. As more water was evaporated, the sol turned into a viscous gel. The resulting gel precursors were pre-calcined at 450°C for 4 hours in air to remove the organic substances. The pre-calcined powders were finally calcined at 900°C for 12 hours in the air, and then furnace-cooled to room temperature to obtain mixed oxide powders.

X-ray diffraction

Powder X-ray diffraction (Rigaku D-max) using $\text{Cu K}\alpha$ radiation was used to identify the crystalline phase of the final oxide powders. The XRD spectra were recorded in a range of 2θ values from 10° to 70° at a scanning rate of 0.5 degrees per min and a step size of 0.02° .

Scanning electron microscope

The morphology of final oxide powders were characterized by scanning electron microscope (SEM, Hitachi, S3000).

Electron Spectroscopy for Chemical Analysis

The X-ray photoelectron spectroscopy (XPS; a PHI VersaProbe 5000 Scanning X-ray Photoelectron Spectrometer) analysis of the samples was performed with monochromatic Al K α (1486.8 eV) radiation as the X-ray source.

Electrochemical Characterization

The cathodes were prepared by mixing the synthesized sample, carbon black and poly-vinylidene fluoride at a weight ratio of 80:10:10 in the solvent of N-methylpyrrolidone. The resulting slurries were cast onto aluminum current collectors and then dried at 100°C under vacuum for 24 hours. The foils were rolled to thin sheets, then cut into disks with a diameter of 13 mm. CR2032 coin-type cells were assembled in an argon-filled glove box, lithium foils were used as counter electrodes, and polypropylene microporous films were used as separators. The electrolyte consisted of 1 M LiPF₆ in a mixture of ethyl carbonate and diethyl carbonate at a 1:1 volume ratio. The galvanostatic charge and discharge tests were carried out on an Arbin testing instrument in a voltage range between 2.0V and 4.8V at various C-rate (15mA/g).

Electrochemical Impedance Spectroscopy

Electrochemical impedance spectroscopy (EIS) was performed using a coin cell after one cycle of charge and discharge. The current of C/10 rate was applied, after which the cell was relaxed for 24 hours to reach the steady state OCV. A sinusoidal amplitude modulation of ± 10 mV was

carried out in a frequency range from 10 MHz to .01 Hz, starting at high frequency and moving toward low frequency in the logarithmic scan. (Autolab PGSTAT30, Eco. Chemie)

Conductivity measurement

The powders were pressed into cylinder-shaped samples (D=8mm, L=10mm) and sintered at 900°C for 12hr to densify the samples. The samples were polished and painted with silver paste on both sides. The resistance of the samples was measured by DC digital multimeter, 34970A/34901A. The conductivity can be calculated by the following equations:

$$\sigma = \frac{1}{R} \times \frac{L}{A} \dots\dots\dots(1)$$

$$\sigma_M = \sigma \frac{1 - v_p}{1 + \frac{1}{2}v_p} \dots\dots\dots(2)$$

σ : conductivity of densified sample R: resistance A: area of the sample

L: length of sample σ_M : conductivity of sample with high porosity

v_p : porosity of sample

Results and Discussion:

1. Phase identification of Mo-doped Li-rich cathode powders

The Mo-doped Li-rich cathode $0.5\text{Li}_2\text{Mn}_{1-x}\text{Mo}_x\text{O}_3-0.5\text{LiNi}_{1/3}\text{Mn}_{1/3}\text{Co}_{1/3}\text{O}_2$ ($x=0, 0.025$ and 0.5) was synthesized through sol-gel method. When $x=0.025$, the cathode material is formulated as $\text{Li}_{1.2}\text{Mn}_{0.531}\text{Ni}_{0.13}\text{Co}_{0.13}\text{Mo}_{0.009}\text{O}_2$. Fig. 2 shows the XRD pattern of the synthesized Mo-doped Li-rich cathode powder. The XRD pattern shows the typical reflections of layered structure without any additional reflections. As the addition of molybdenum increase to $x=0.05$, the diffracted reflections of impurity phase was observed at 2θ angle around $28\sim 35$ degree. The impurity phase was identified as MoO_3 . The lattice constant of the Mo-doped Li-rich cathode is listed in Table.1 The lattice constant of $0.5\text{Li}_2\text{MnO}_3-0.5\text{LiNi}_{1/3}\text{Mn}_{1/3}\text{Co}_{1/3}\text{O}_2$ increased from 2.8651 \AA to 2.8685 \AA after Molybdenum doping. This may be caused by the larger ionic radius of Mo^{+6} (0.59 \AA) than that of Mn^{+4} (0.54 \AA). Both lattice constant and volume increase as the content of Mo increase. The

maximum solubility of Mo in Li-rich cathode is found to be less than 1% similar to the work of Zang et al [5].

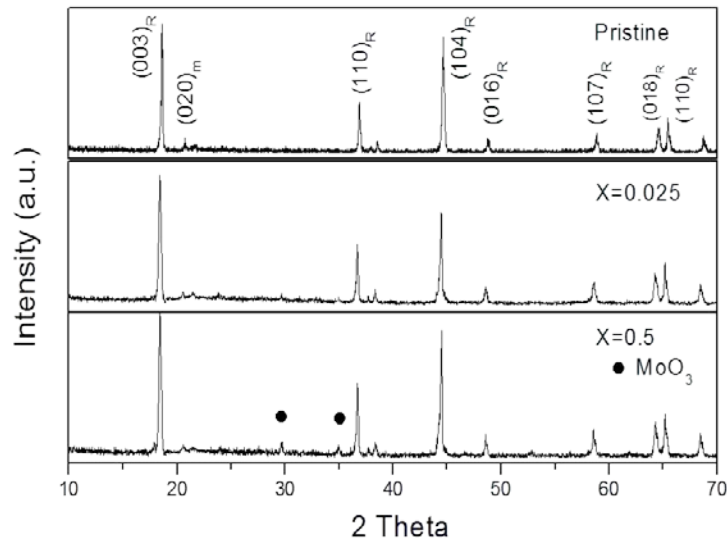


Fig.2 XRD pattern of $0.5\text{Li}_2\text{Mn}_{1-x}\text{Mo}_x\text{O}_3-0.5\text{LiNi}_{1/3}\text{Mn}_{1/3}\text{Co}_{1/3}\text{O}_2$ ($x=0, 0.025$ and 0.5) synthesized through sol-gel method

Table. 1 Lattice parameter of $0.5\text{Li}_2\text{Mn}_{1-x}\text{Mo}_x\text{O}_3-0.5\text{LiNi}_{1/3}\text{Mn}_{1/3}\text{Co}_{1/3}\text{O}_2$ ($x=0, 0.025$ and 0.5) synthesized at 900°C in air for 6hr

	a (Å)	c (Å)	V(Å ³)
X=0	2.8651	14.25194	101.3036
X=0.025	2.8668	14.2516	101.4275
X=0.05	2.8685	14.25195	101.5579

2. SEM image and XPS analysis of Mo-doped Li-rich cathode

The SEM image and EDX mapping of $x=0.025$ Li-rich cathode are shown in Fig.3 The particle size of the synthesized powder was analyzed to be in a range between 200 and 300nm. EDX mapping result of Mn, Co, Ni and Mo indicated that all the metal ions distributed homogeneously in the cathode powder. The XPS analysis of Mo-3d orbital of the Mo-doped Li-rich cathode is shown in

Fig. 4. The binding energy of Mo^{+5} based on the XPS analysis of Mo from the work of Co-PI, Prof. Meng et al [6] was reported to be 231.7 eV in $3d_{5/2}$ and 234.8eV in $3d_{3/2}$. The binding energy of Mn^{+4} and Mn^{+3} is 644.6 and 640.6eV respectively [7]. The fitting result of Mo revealed that around 48% of Mo is Mo^{+6} and 52% of Mo is in +5 valence state. Base on electrical neutrality, it's calculated that 2.31% of Mn^{+4} will be reduced to Mn^{+3} . Fig. 4 shows the Mn 2p XPS result of $0.5\text{Li}_2\text{Mn}_{1-x}\text{Mo}_x\text{O}_3-0.5\text{LiNi}_{1/3}\text{Mn}_{1/3}\text{Co}_{1/3}\text{O}_2$ ($x=0$ and 0.025). In pristine (undoped) Li-rich cathode, the valence state of Mn is mainly Mn^{+4} . After Mo is introduced into $0.5\text{Li}_2\text{Mn}_{1-x}\text{Mo}_x\text{O}_3-0.5\text{LiNi}_{1/3}\text{Mn}_{1/3}\text{Co}_{1/3}\text{O}_2$, $\text{Mn}^{+3}:\text{Mn}^{+4}$ was estimated to be 2.17%: 97.83% based by the fitting result of Mn 2d XPS spectra. This result is consistent with the value estimated from Mo valence. The measured conductivities of undoped and Mo-doped Li-rich cathode are listed in Table. 2. The conductivity of pristine (undoped) Li-rich cathode is around 3.43×10^{-8} s/cm. After Mo was introduced to the Li-rich cathode, its conductivity was enhanced to 7.018×10^{-7} S/cm being 50 times higher than undoped one. The increase in conductivity is attributed to the presence of $\text{Mn}^{+3}/\text{Mn}^{+4}$ in the cathode.

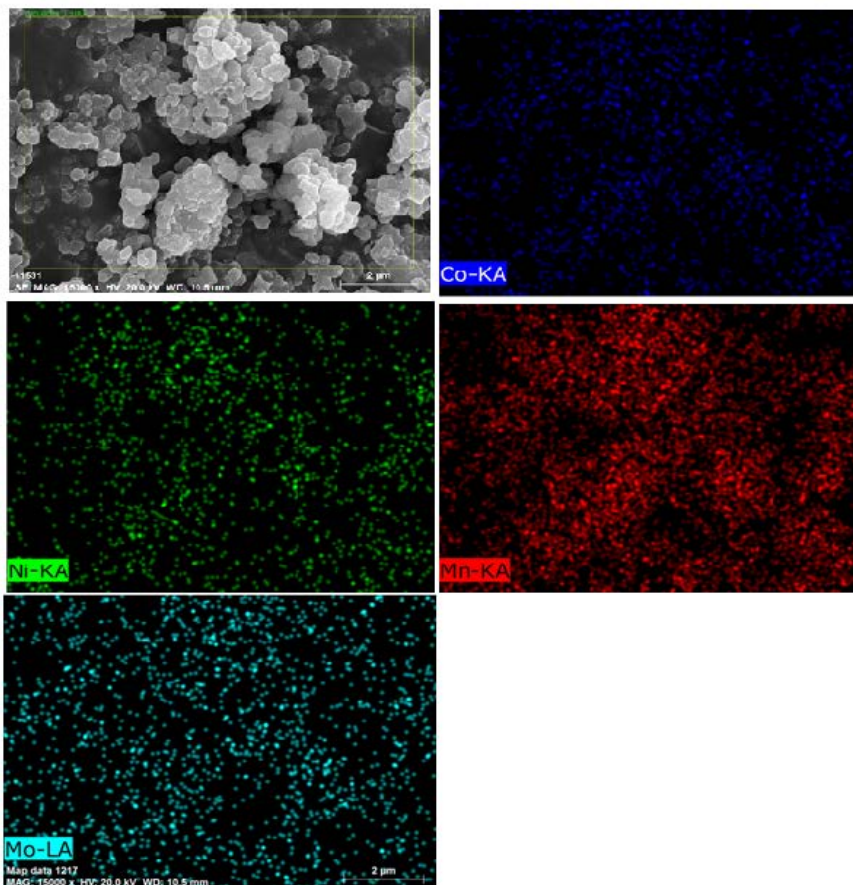


Fig.3 SEM image of $0.5\text{Li}_2\text{Mn}_{1-x}\text{Mo}_x\text{O}_3-0.5\text{LiNi}_{1/3}\text{Mn}_{1/3}\text{Co}_{1/3}\text{O}_2$ ($x=0.025$) powder

prepared by sol-gel method and EDX mapping of Co, Ni, Mn and Mo

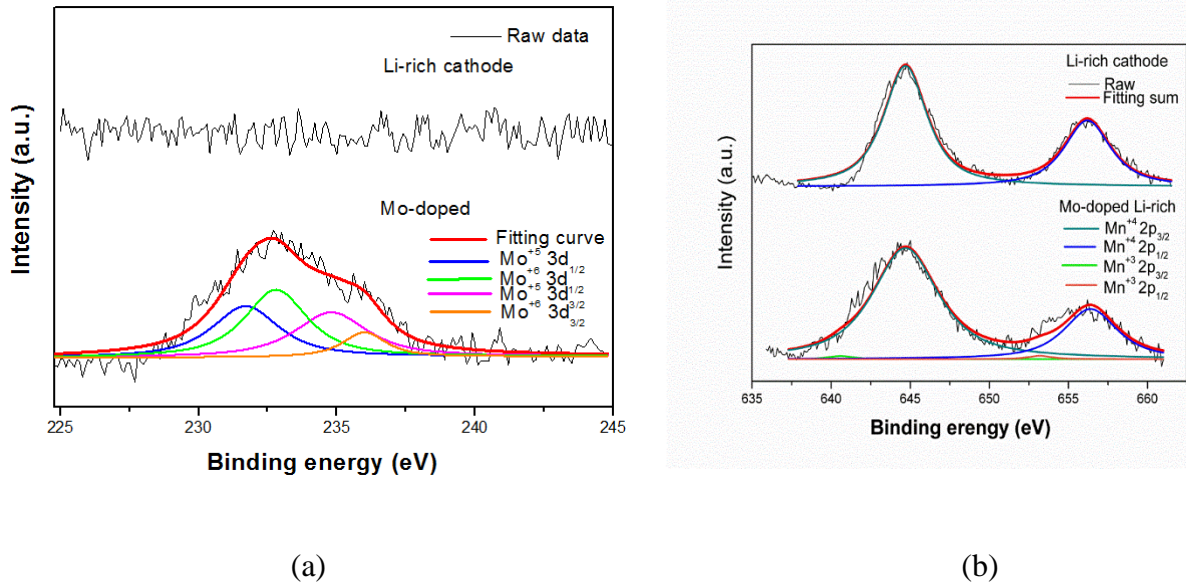


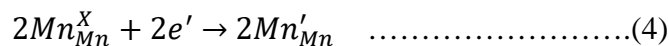
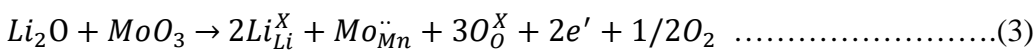
Fig.4 (a) Mo 3d and (b) Mn 2p orbital XPS analysis of $0.5\text{Li}_2\text{Mn}_{1-x}\text{Mo}_x\text{O}_3-0.5\text{LiNi}_{1/3}\text{Mn}_{1/3}\text{Co}_{1/3}\text{O}_2$ ($x=0$ and 0.025)

Table2. Conductivity and Density of NMC and $0.5\text{Li}_2\text{Mn}_{1-x}\text{Mo}_x\text{O}_3-0.5\text{LiNi}_{1/3}\text{Mn}_{1/3}\text{Co}_{1/3}\text{O}_2$ ($x=0$ and 0.025)

Composition	Density (g/cm ³)	Relative density (%)	Porosity (%)	Conductivity (s/cm)
(b) $\text{Li}_{1.2}\text{Mn}_{0.54}\text{CO}_{0.13}\text{Ni}_{0.13}\text{O}_2$	3.13	74.4	25.54	3.34×10^{-8}
(c) $\text{Li}_{1.2}\text{Mn}_{0.532}\text{Mo}_{0.085}\text{CO}_{0.13}\text{Ni}_{0.13}\text{O}_2$	3.419	81.1	18.83	7.018×10^{-7}

3. Electrochemical performance of Mo-doped Li-rich cathode

The first charge curve of $0.5\text{Li}_2\text{Mn}_{1-x}\text{Mo}_x\text{O}_3-0.5\text{LiNi}_{1/3}\text{Mn}_{1/3}\text{Co}_{1/3}\text{O}_2$ ($x=0$ and 0.025) is shown in Fig.5. For charging voltage greater than 3.8V, Mo-doped cathode shows higher capacity than undoped one. Such charging behavior is typically observed in the cathode with higher electrical conductivity. For understanding of doping effect, the following defect reactions may be derived:



Based on reaction (3), the replacement of one Mo^{+6} for Mn^{+4} will induce the formation of two electrons. After two electrons are associated with Mn^{+4} , Mn ions will be reduced to Mn^{+3} .

The discharge capacity for samples ($x=0$ and 0.025) was 245mAh/g and 269mAh/g respectively. The increase in capacity may be well explained by the presence of more Mn^{+3} ions in Mo-doped sample. In Mo-doped samples, the induced Mn^{+3} may release an electron and become Mn^{+4} during the charge state. But in the undoped sample, the Mn remains Mn^{+4} in the charge state, result in lower capacity. The voltage plateau of the pristine (undoped) Li-rich cathode is around 4.5V . But the voltage plateau drop to 4.43V in $x=0.025$ sample. The phenomenon can be explained by the higher conduction of Mo-doped sample. The lower ohmic loss in the more conducting cathode enhances Li insertion/extraction.

Fig.6 (a) shows the cyclic performance of the Li-rich cathode synthesized by sol-gel method ($0.5\text{Li}_2\text{Mn}_{1-x}\text{Mo}_x\text{O}_3-0.5\text{LiNi}_{1/3}\text{Mn}_{1/3}\text{Co}_{1/3}\text{O}_2$ ($x=0$ and 0.025)) at 0.05C for 30 cycles. The Mo-doped samples exhibited 269mAh/g in first discharge capacity, while the sample without Mo-doping was only 245.4mAh/g . Table.3 shows the list of charge/discharge capacity in the first cycle. Doping Mo into the Li-rich cathode can reduce the irreversible capacity loss and increase the columbic efficiency. The irreversible capacity loss of undoped sample was 81.26mAh/g , while the $x=0.025$ only showed 46.925mAh/g of irreversible capacity loss. The columbic efficiency also increased from 75.05% to 85.15% after Mo addition into the Li-rich cathode. The discharge capacity under different C-rate test is shown in Fig. 6 (b). Under low C-rate (0.05C), the discharge capacity of Li-rich cathode prepared by sol-gel method and Mo-doped is around 245 and 269mAh/g respectively. The discharge capacity of sol-gel method powder dropped to 140mAh/g as the C-rate increase to 0.5C , while the Mo-doped sample exhibit 175mAh/g . In high C-rate, the Mo-doped sample can deliver the higher capacity than undoped one. This can be attributed to the conductivity enhancement caused by Mo-induced additional electrons. Cathode with higher conductivity significantly reduces the ohmic loss. Thus, its charge/discharge capacity tends to be higher under high C-rate. The cyclic performance of Mo-doped is also more improved than the undoped one using sol-gel method. The stronger Mo-O bond in Mo-doped sample also enhances the structure stability and supresses the capacity degradation in comparison to the un-doped one. Fig. 7 shows the EIS result of the $0.5\text{Li}_2\text{Mn}_{1-x}\text{Mo}_x\text{O}_3-0.5\text{LiNi}_{1/3}\text{Mn}_{1/3}\text{Co}_{1/3}\text{O}_2$ ($x=0, 0.025$ and 0.05) cathode. The equivalent circuit shows there are four main resistances in the coin cell: (1) Resistance of electrolyte (R_e) (2) Resistance between the interfaces (R_i) (3) Charge transfer resistance (R_{ct}) (4) Warburg Impedance (Z_w), which is related to the lithium ion diffusion coefficient (D_{Li}) in the electrode. The fitting result of the resistance in the equivalent circuit is listed in Table. 4. The

resistance of electrolyte (R_e) and resistance between the interfaces (R_i) of all the tested samples was almost the same. The value of charge transfer resistance (R_{ct}) was extracted from the semicircle at the high frequency by fitting into the equivalent circuit model. The R_{ct} value of the Mo-doped samples showed noticeable differences. In pristine (undoped) Li-rich cathode, the R_{ct} is 602Ω . After Mo-doping ($x=0.025$ and 0.05), R_{ct} decreased to 132Ω and 313Ω . It is expected that Mo-doped cathode with reduced charge transfer resistance tends to better electrons exchange in the electrode. This is also the reason why the Mo-doped sample exhibited higher discharge capacity in high C-rate (Fig.6 (b).) The R_{ct} of $x=0.05$ was larger than $x=0.025$ because some impurity phase (MoO_3) exist in the cathode result in higher R_{ct} .

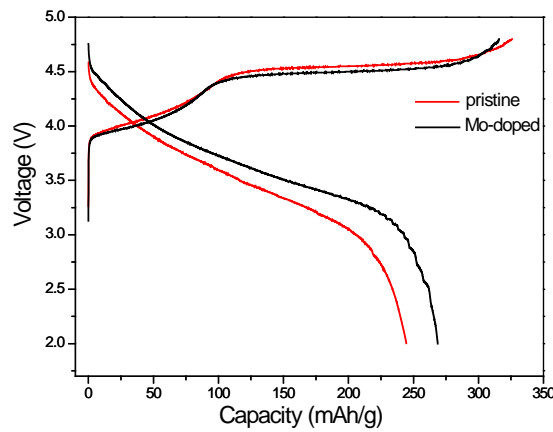


Fig.5 Charge-discharge curve of Mo-doped Li-rich cathode at 0.05C between 2~4.8V

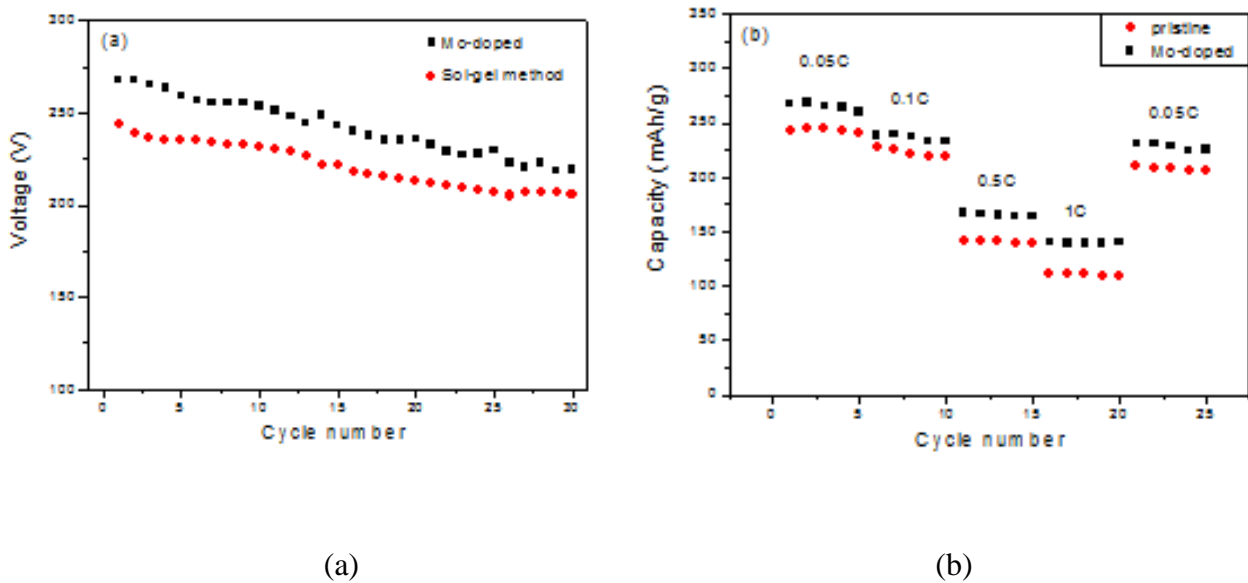


Fig. 6 (a) Cyclic performance of $0.5Li_2Mn_{1-x}Mo_xO_3-0.5LiNi_{1/3}Mn_{1/3}Co_{1/3}O_2$ ($x=0$ and 0.025) at $0.05C$ between $2\sim 4.8V$ (b) Cyclic performance at different C-rate ($0.05C\sim 1C$)

Table. 3 1stcharge/discharge capacity and columbic efficiency of 0.5Li₂Mn_{1-x}Mo_xO₃-0.5LiNi_{1/3}Mn_{1/3}Co_{1/3}O₂ (x=0 and 0.025)

Content of Molybdenum	First charge capacity(mAh/g)	First discharge capacity(mAh/g)	Irreversible capacity loss(mAh/g)	Columbic efficiency
X=0	325.8	244.54	81.26	75.05%
X=0.025	315.925	269	46.925	85.15%

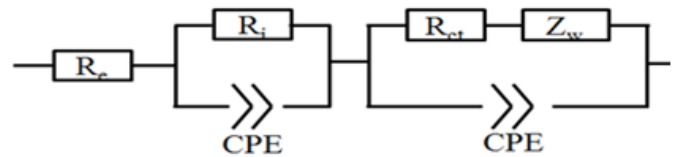
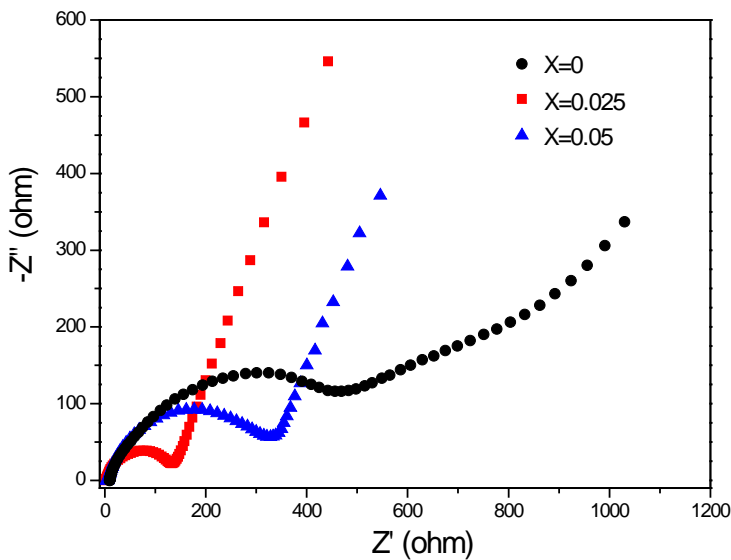


Fig. 7 Nyquist plots of 0.5Li₂Mn_{1-x}Mo_xO₃-0.5LiNi_{1/3}Mn_{1/3}Co_{1/3}O₂ (x=0, 0.025 and 0.05) cell and schematic diagram of the equivalent circuit used for fitting the coin cell electrodes

Table. 4 Fitting result of parameter R_e, R_i and R_{ct} in the equivalent circuit

	R _e (Ω)	R _i (Ω)	R _{ct} (Ω)
X=0	2.605	33.14	602
X=0.025	2.581	32.75	132
X=0.05	2.594	33.61	313

Conclusions

1. The Mo-doped Li-rich cathode $0.5\text{Li}_2\text{Mn}_{1-x}\text{Mo}_x\text{O}_3-0.5\text{LiNi}_{1/3}\text{Mn}_{1/3}\text{Co}_{1/3}\text{O}_2$ ($x=0, 0.025$ and 0.05) were prepared through sol-gel method. Impurity identified as MoO_3 showed in the $x=0.05$ sample. The XPS analysis of Mo in the Li-rich cathode ($x=0.025$) shows that the ratio of Mo^{+5} : Mo^{+6} = 52%:48%. The XPS analysis of Mn also shows reduction from Mn^{+4} to Mn^{+3} . As a result, the bulk conductivity of the Mo-doped Li-rich cathode is also enhanced.

2. In Mo-doped samples, the induced Mn^{+3} tends to release an electron and become Mn^{+4} during the charge state. As the Mo content increase, the charge capacity of Mo-doped Li-rich cathode increases due to the enhanced conduction caused by the presence of Mn^{+3} . The irreversible capacity loss of undoped sample was 81.26mAh/g, while the $x=0.025$ only showed 46.925 mAh/g of irreversible capacity loss. The columbic efficiency also increased from 75.05% to 85.15% after Mo addition into the Li-rich cathode. The cyclic performance of Li-rich cathode was also enhanced because of strong Mo-O bonding.

3. Under high C-rate, the Mo-doped sample deliver the higher rate-capability than the undoped one. This result may be attributed to the enhancement in electronic conduction after Mo-doping. Cathode with higher conductivity significantly reduces the ohmic loss. Thus, its charge/discharge capacity tends to be higher under high C-rate. High conductivity makes electron exchange earlier inside the materials, thus the charge/discharge capacity can be increased in high C-rate. Furthermore, the fitting result of EIS measurement also demonstrate that the charge transfer resistance (R_{ct}) of Mo-doped sample is smaller than that of the pristine (undoped) sample.

References

[1] Lu, Z.; MacNeil, D. D.; Dahn, J. R. *Electrochem. Solid-State Lett.*, 4, A191 (2001)

- [2] J. S. Kim, C. S. Johnson, J. T. Vaughey; M. M. Thackeray, S. A. Hackney; W. Yoon, C. P. Grey, *Chem. Mater.* 16, p. 1996-2006 (2004).
- [3] Z. Lu, J. R. Dahn, *J. Electrochem. Soc.* 149 (7) A815-A822 (2002).
- [4] B. Xu, C. R. Fell, M. Chic and Y. S. Meng, *Energy Environ.* 4, p. 2223–2233 (2004).
- [5] Y. Zang, C.-X. Ding, X.-C. Wang, Z.-Y. Wen, and C.-H. Chen, *Electrochimica Acta*, vol. 168, pp. 234-239, 2015/06/20/ 2015.
- [6] X. Deng, S. Y. Quek, M. M. Biener, J. Biener, D. H. Kang, R. Schalek, E. Kaxiras, C. M. Friend, X. Deng, S. Y. Quek, M. M. Biener, J. Biener, D. H. Kang, R. Schalek, E. Kaxiras, and C. M. Friend, *Surf. Sci.*, vol. 602, no. 6, pp. 1166–1174, 2007.
- [7] L. Xiao *et al.*, "Effects of structural defects on the electrochemical activation of Li_2MnO_3 ," *Nano Energy*, vol. 16, pp. 143-151, 9// 2015.

List of Publications and Significant Collaborations that resulted from your AOARD

supported project: In standard format showing authors, title, journal, issue, pages, and date, for each category list the following:

(i) Conference papers

1. K. Z. Fung, S. Y. Tsai, C. T. Ni, W. Z. Lin, and B. Y. Huang, Effect of Phase Transformation on Electrochemical Properties of Li-rich $x\text{Li}_2\text{MO}_3$ - (1-x) LiMO_2 composite cathode for high capacity Li ion batteries, 2017 Annual Meeting of the Taiwan Ceramic Society, May 19, 2017
2. K. Z. Fung, C. Ni, S. Y. Tsai, B. Y. Huang, , "Effect of Structural Evolution on Electrochemical Properties of Li-Rich Layered Oxide Cathode" 15th International Conference on Advanced Materials, IUMRS-ICAM 2017, Kyoto Univ, August 27, 2017
3. K. Z. Fung, D. B. Su, B. Y. Huang, S. Y. Tsai, "Behavior of Electrode/Solid Electrolyte Materials for Li Batteries viewing from Defect Considerations", International Battery Association 2018 Meeting, March 11, 2018

(ii) Journal Publication

4. T. A. Wynn, C. C. Fang, M. H. Zhang, H. D. D. Liu, D. M. Davies, X.F. Wang, D. Lau, J. Z. Lee, K.Z. Fung, Y. S. Meng, "Mitigating oxygen release in anionic-redox-active cathode materials by

Appendix

Abstracts for Papers

Abstract #1

Effect of Phase Transformation on Electrochemical Properties of Li-rich $x\text{Li}_2\text{MO}_3\text{-}(1-x)\text{LiMO}_2$ Composite Cathode for High Capacity Li ion Batteries

K. Z. Fung, S. Y. Tsai, C. T. Ni, W. Z. Lin, and B. Y. Huang Department of Materials Science and Engineering, National Cheng Kung University, Tainan, Taiwan,

Recently, Li-rich layered oxides have become attractive cathode materials for their high storage energy applications. Lithium-rich layered oxides materials, represented by the general formula $x\text{Li}_2\text{MnO}_3\cdot(1-x)\text{LiMO}_2$ in which M is Mn, Ni and Co are of interest for both high-power and high capacity lithium-ion cells. To overcome capacity fading problem in Li-rich cathode, Mo-doping was chosen to improve the conductivity, electrochemical performance and stabilized the structure of Li-rich cathode in the study. $\text{Li}_2\text{Mn}_{1-x}\text{Mo}_x\text{O}_3$ ($x=0, 0.025, 0.05$ and 0.1) were synthesized by sol-gel method to investigate their structure and electrochemical properties. The electrochemical test showed that the Mo-doped sample exhibited the highest cycling discharge and cycling performance among the test samples. $X=0.025$ sample exhibited 269mAh/g in the first discharge capacity and remained 224mAh/g after 30cycles. While the undoped one shows 244.5mAh/g in the first cycle and then decayed to 202mAh/g after 30cycles. In addition, Mo-doped Li-rich cathode show more stable cycling performance than the undoped one. The capacity retention rate of Li-rich cathode could be enhanced from 61.23% (sol-gel method) to 82.49% (two step sol-gel method). The AC impedance result proves that the R_{ct} (charge transfer resistance) was reduced after Mo-doping. Such improvement may be also the reason why the Mo-doped sample exhibited the enhanced capacity performance, especially at high C-rate.

Abstract #2

Effect of Structural Evolution on Electrochemical Properties of Li-Rich Layered Oxide Cathode

*K.-Z. Fung^{1,2)}, C. Ni²⁾, S.-Y. Tsai¹⁾, and B.-Y. Huang¹⁾

1) Department of Materials Science and Engineering, National Cheng Kung University, Tainan, Taiwan, 2) Research Center for Energy Technology and Strategy (RCETS), National Cheng Kung University

*z8702009@email.ncku.edu.tw

Cathode materials formulated as $x\text{Li}_2\text{MnO}_3\text{-}(1-x)\text{LiMO}_2$ ($M = \text{Mn, Ni, Co, etc.}$) showing layer-structure received much attention due to their surprisingly high reversible capacity for Li-ion battery applications.[1,2] For better understanding of such high-capacity layered cathode, a systematic study on powder morphology, crystal structures and reaction mechanisms of $\text{Li}_{1.2}\text{Mn}_{0.54}\text{Ni}_{0.13}\text{Co}_{0.13}\text{O}_2$ during electrochemical charge/discharge cycles were conducted. First, the capacity of Li-rich layered cathode powder was strongly affected by its particle size. To obtain various particle sizes of cathode powder, different powder synthesis routes have been

adopted. By using sol-gel process, particle size of $\text{Li}_{1.2}\text{Mn}_{0.54}\text{Ni}_{0.13}\text{Co}_{0.13}\text{O}_2$ powder obtained is around 200 nm. On the other hand, $\text{Li}_{1.2}\text{Mn}_{0.54}\text{Ni}_{0.13}\text{Co}_{0.13}\text{O}_2$ powder synthesized by solid-state reaction method gives particle size as coarse as $1.0\mu\text{m}$. As a result shown in Fig.1, the initial discharge capacity of sol-gel processed Li-rich cathode was 250 mAh/g. After 40 cycles, the discharge capacity from the same cathode still shows a capacity as high as 205 mAh/g. However, for cathode powder from solid-state reaction, its initial capacity was 190 mAh/g that is 24% lower than that of sol-gel processed cathode. After 40 cycles, the capacity degraded to 137 mAh/g. The enhanced capacity of sol-gel processed Li-rich cathode is attributed to its enormous surface area and short Li diffusion distance provided for electrochemical reaction to take place.

Although Li-rich layer-structured cathode material show a reversible capacity as high as 250 mAh/g at low rate, its electrochemical properties such as capacity loss at first cycle, rate capability and capacity fading still need to be examined and characterized. In this study, $\text{Li}[\text{Li}_{0.2}\text{Mn}_{0.54}\text{Ni}_{0.13}\text{Co}_{0.13}]\text{O}_2$ were investigated. The TEM structural analysis shows that the evidence of spinel phase after cycling. It is believed that the transition from layered structure to spinel structure may also induce a large lattice distortion resulting in lattice breakdown and capacity fading. In addition, the phase transition may be caused by the redox reaction of transition metal ions through charging/discharging tests.

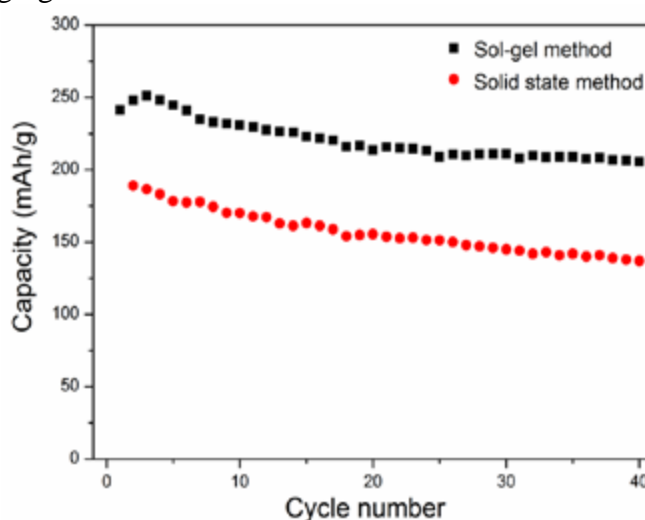


Fig.1. Cycling performance of $\text{Li}_{1.2}\text{Mn}_{0.54}\text{Co}_{0.13}\text{Ni}_{0.13}\text{O}_2$ prepared by sol-gel and solid-state reaction methods at 0.1C between 2-4.8V

References:

- 1) Y. Xu, E. Hu, F. Yang, J. Corbett, Z. Sun, Y. Lyu, X. Yu, Y. Liu, X.-Q. Yang and H. Li, *Nano Energy* 28, 164 (2016),
- 2) P. Rozier and J. M. Tarascon, *J. Electrochem. Soc.*, 162, [14], A2490-A2499 (2015)

Abstract #3

BEHAVIOR OF ELECTRODE/SOLID ELECTROLYTE MATERIALS FOR LI BATTERIES VIEWING FROM DEFECT CONSIDERATIONS

Kuan-Zong Fung^{1,2}, Dong-Bow Su¹, Bo-Yuan Huang¹, Shu-Yi Tsai²

¹Department of Materials Science and Engineering, National Cheng Kung University,
Tainan, TAIWAN

²Research Center for Energy Technology and Strategy (RCETS), National Cheng
Kung University, Tainan, TAIWAN
E-mail: z8702009@email.ncku.edu.tw

Functional oxides are widely used for lithium battery applications. Their electrochemical properties are typically highly dependent on their defect structures.

For examples, the capacity of Li-rich layer-structured cathode formulated as $x\text{Li}_2\text{MnO}_3-(1-x)\text{LiMO}_2$ ($M = \text{Mn, Ni, Co, etc.}$) was able to provide high reversible capacity ($>250 \text{ mAh/g}$) for Li-ion battery applications due to the combined effect of oxygen oxidation, vacancy formation and followed by manganese reduction (or activation). Furthermore, the zero-strain anode materials $\text{Li}_4\text{Ti}_5\text{O}_{12}$ shows high interface polarization and low rate capability due to low electronic conduction. Hopefully, the capacity and rate capability may be improved by introduction of electronic defects on Ti cation sublattice.

In additions, the properties of solid state Li ion conductors for all-solid-state lithium batteries is strongly affected by their defect structures as well. Due to its better safety characteristics, solid-state lithium battery may use highly reactive anode, such as Li. Thus, it is extremely crucial to find a stable solid electrolyte when the high-capacity Li anode is used.

In our study, the stability of perovskite-based $\text{La}_{0.50}\text{Li}_{0.50}\text{TiO}_3$, NASICON-based Al-doped $\text{LiTi}_2(\text{PO}_4)_3$, and garnet-based $\text{Li}_7\text{La}_3\text{Zr}_2\text{O}_{12}$ against metallic Li were investigated. After $\text{La}_{0.50}\text{Li}_{0.50}\text{TiO}_3$ reacted with Li, the electron injection accompanied by the incorporation (insertion) of Li ion into vacant cation sites was likely to take place. The apparent reduction of tetravalent Ti into trivalent Ti was observed in $\text{La}_{0.50}\text{Li}_{0.50}\text{TiO}_3$. On the other hand, Al-doped $\text{LiTi}_2(\text{PO}_4)_3$, and garnet-based $\text{Li}_7\text{La}_3\text{Zr}_2\text{O}_{12}$ are much more stable when Li anode is used. For these solid electrolytes, the difference in stability against metallic Li may be rationalized based on their defect structures and corresponding atomic arrangements.

Abstract #4

Mitigating Oxygen Release in Anionic-Redox-Active Cathode Materials by Cationic Substitution through Rational Design

Thomas A. Wynn^{a,○}, Chengcheng Fang^{a,○}, Minghao Zhang^b, Haodong D. Liu^b, Daniel M. Davies^b, Xuefeng Wang^b, Derek Lau^b, Jungwoo Z. Lee^b, Kuan-Zong Fung^c, Ying Shirley Meng^{a, b,*}

a. Materials Science and Engineering Program, University of California San Diego,
La Jolla, CA 92037, USA.

b. Department of NanoEngineering, University of California San Diego, La Jolla, CA

92037, USA.

c. Department of Materials Science and Engineering, National Cheng Kung University, Tainan 70101, Taiwan, ROC

° Equal authorship

* Corresponding Author, E-mail: shirleymeng@ucsd.edu

Through the incorporation of excess lithium in the transition metal layer, the role of oxygen has extended beyond its essential role as a structural component in classical layered oxide cathodes, exhibiting electrochemical activity and enhancing the reversible capacities of layered oxides through anionic redox mechanisms. Commensurate with the enhanced activity of the oxygen comes its instability in the form of oxygen loss, which is associated with irreversible voltage decay and capacity fade. To develop an understanding of this irreversible loss and to increase the stability of lattice oxygen, density functional theory is applied to calculate oxygen vacancy formation energies, $E_{O_v}^F$, in lithium rich transition metal layered oxides for a variety of dopants, noting an increased stability upon doping of 4d elements Mo and Ru. Motivated by these findings, representative dopants Al, Ti, and Co are doped into Li-rich NiMn layered oxide $\text{Li}_{1.2}\text{Ni}_{0.2-x/2}\text{Mn}_{0.6-x/2}\text{M}_x\text{O}_2$, with dopant (M) concentrations ranging from 1–13%, showing behavior consistent with the prediction by calculations, and similarly Mo is co-doped with Co, showing notably reduced voltage decay and capacity fade without sacrificing energy density and cycle life. Calculations suggest this is due to a modified charge density distribution around oxygen anions upon incorporation of Mo, altering local band structure and impeding oxygen vacancy formation, while maintaining the oxygen activity for reversible redox.

DD882: As a separate document, please complete and sign the inventions disclosure form.

Important Note: If the work has been adequately described in refereed publications, submit an abstract as described above but cite important findings to your above List of Publications, and if possible, attach any reprint(s) as an appendix. If a full report needs to be written, then submission of a final report that is very similar to a full length journal article will be sufficient in most cases.